Pergamon

Tetrahedron 58 (2002) 5849–5854

TETRAHEDRON

Synthesis and characterization of 4,7-dimethyl-1,4,7,10,15,18-hexaazabicyclo[8.5.5]octane. Crystal structures of the cryptate and of the first small azacage complexes with six-coordinate lithium geometry

Mircea Vlassa,[a,*] Ruy Huang,[b] James E. Jackson[b] and James L. Dye[b]

[a]*Department of Organic Chemistry, Faculty of Chemistry and Chemical Engineering, Babes-Bolyai University, 11 Arany Janos street, RO-3400, Cluj-Napoca, Romania*

[b]*Department of Chemistry, Michigan State University, East Lansing, MI 48824, USA*

Received 25 February 2002; revised 14 May 2002; accepted 30 May 2002

Abstract—The synthesis and characterization of 4,7-dimethyl-4,7,10,11,15, 18-hexaazabicy-clo[8.5.5]octane (**L**) is described. The ligation properties of the macrobicyclic ligand towards alkaline metal cations are considered. The crystalline structures of the ligand **L** and of the first small azacage complexes with six-coordinate lithium geometry, $[Li\mathbf{L}]^+[BPh_4]^-$and $[Li\mathbf{L}]^+[ClO_4]^-$, are presented. © 2002 Published by Elsevier Science Ltd.

1. Introduction

The problem of thermal stability of alkalides and electrides is crucial for the potential practical applications.[1] One way to achieve greater thermal stability is to obtain compounds which are more resistant to reduction. The use of aza-cryptands, which have a very high complexing power, resulted in the synthesis of the most stable alkalide toward decomposition with no apparent tendency toward decomplexation.[2]

The synthesis and application of these robust complexes are a major goal of alkalide and electride research. Taking into consideration the above-mentioned facts, we are interested in the preparation of new azacryptands, selective for lithium encapsulation, more resistant to reduction.

2. Results and discussion

In the present paper, we report the synthesis, characterization and ligation properties of the title compound, hereafter abbreviated as **L**. Reaction of macrocycle **1** with tosylate **2** generated cryptand **3**, which on deprotection with H_2SO_4 gave the desired ligand **L** (see Scheme 1).

The yield of cryptand formation depends upon the concentration of the reactants, the best one (70%) was achieved when a 0.092 M solution of **1** in acetonitrile was treated with one equivalent of a 0.031 M solution of **2** in the same solvent (see Section 3).

Compound **L**, due to the presence of two secondary amino groups is a versatile synthon for preparation of new compounds such as alkylated derivatives (e.g. compound **4** see Scheme 1) or macrotricyclic derivatives by ring closing reactions.

The compounds were fully characterized by, NMR, MS, IR and elemental analysis (see Section 3). The ^{13}C NMR spectra of **L** contains six resonances. The occurrence of only six suggests **L** possesses C_{2v} symmetry, possible a time average of lower-symmetry conformers and/or tautomers.

One specific characteristic of this macrocyclic cage is the selective encapsulation of the Li^+ cation. With alkali metal NMR spectroscopy as a diagnostic technique, no evidence was found for the complexation of Na^+ or K^+. With the lithium ion, solid complexes were isolated and characterized (see Section 3). Li^+ is encapsulated by **L** and the equilibrium (1) was investigated by measuring the ^7Li NMR spectrum of the complex.

$$L(aq) + Li^+(aq) = [LLi]^+(aq) \quad (1)$$

The ^7Li NMR spectra of the complex in water at high pH values, shows a sharp signal at +0.840 ppm, this is shifted downfield with respect to the solvated Li^+ (+0.402 ppm).

Keywords: aza compounds; cage compounds; cryptands; X-ray crystal structure.

* Corresponding author. Tel.: +40-64-193833; fax: +40-64-190818; e-mail: mvlassa@chem.ubbcluj.ro

0040–4020/02/$ - see front matter © 2002 Published by Elsevier Science Ltd.
PII: S0040-4020(02)00562-8

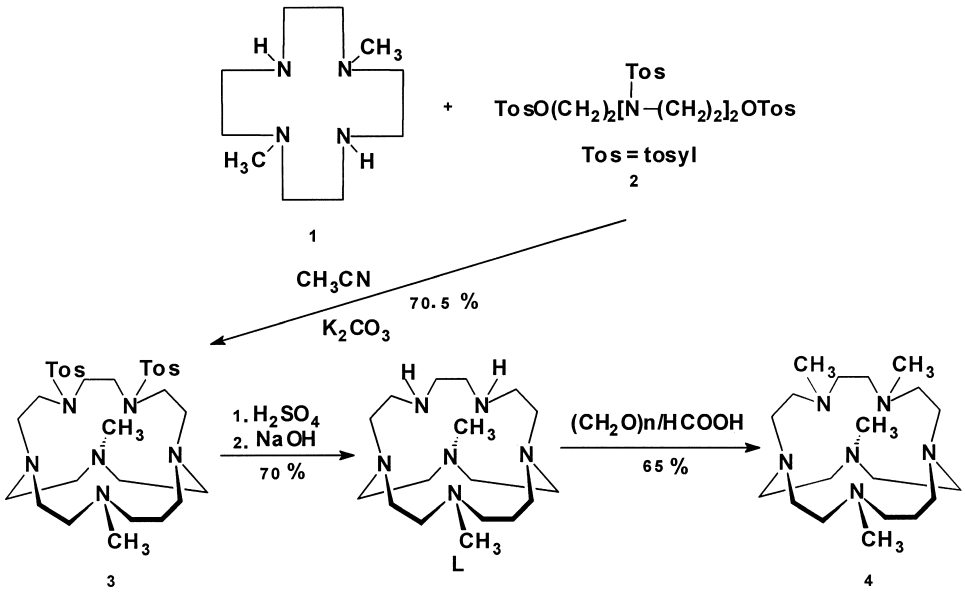

Scheme 1.

The difference ($\Delta\delta$=0.438 ppm) between complex and solvated Li^+, even in such a highly solvating solvent such as water, is similar to shifts found previously for other cryptands[3] and shows that the complex is stable (see Fig. 1). The NMR spectrum of Li^+ in methanol in the presence of L shows that all the cations are bound and this is indicative of a higher stability constant in this solvent.

At room temperature, at equilibrium, only 33.66% of the Li^+ is encapsulated but at 80°C this rises to 78.76%. The stability constants calculated from peak area of ^{7}Li NMR spectra are log K=2.49 (water at room temperature) and 3.85 (water at 80°C). These values indicate a good ability of **L** to encapsulate lithium, but lower in comparison to another small aza-cryptand with one secondary amino group in the bridge, namely 4,10-dimethyl-1,4,7,10,15-penta-azabicyclo[5.5.5]pentane (log K=4.8, determinated in the presence of KOH), prepared by Micheloni and co-workers.[4,5]

In the case of azacryptands, the entropic contribution to the overall reaction spontaneity is much more important than the enthalpic contributions.[6] In the $[LiL]^+$ complex, insertion of the lithium ion into the hydrophobic cavity requires the removal of all the water molecules that surround the free Li^+ ion in aqueous solution. By raising the temperature at 80°C encapsulation of Li^+ is favored by entropic factors. In methanol (ε=32.7), where the lithium cation is less solvated because the charge–dipole interactions are weaker than in water (ε=78.5), the encapsulation is complete.[7] The alkali metal NMR experiments showed that lithium complex formation is not influenced by the presence of Na^+ ions, even in high concentrations, indicating that **L** is able to discriminate between Li^+ and Na^+.

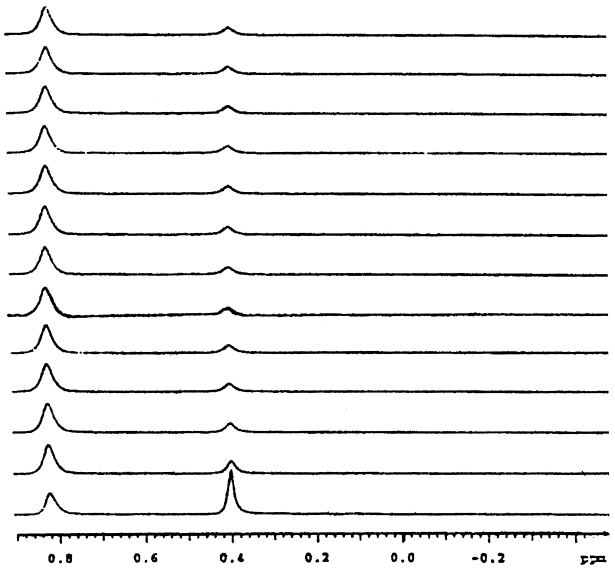

Figure 1. ^{7}Li NMR spectra, taken at 10 min intervals, after mixing an aqueous solution of LiOH (0.05 mol dm^{-3}) with **L** (0.25 mol dm^{-3}) at 80°C.

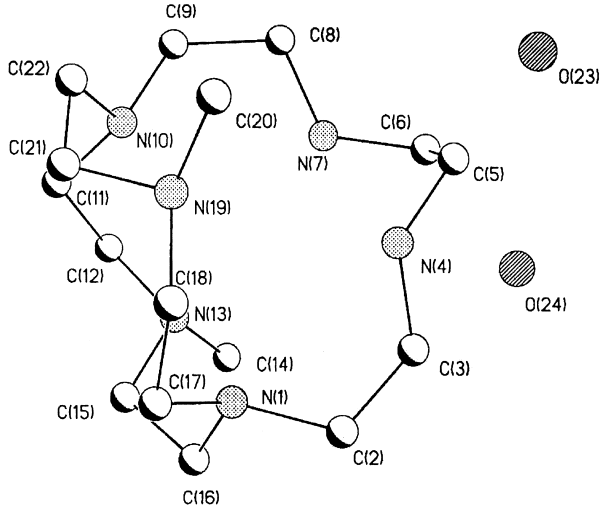

Figure 2. Crystal structure of **L**·2H_2O. Hydrogen atoms have been omitted for clarity.

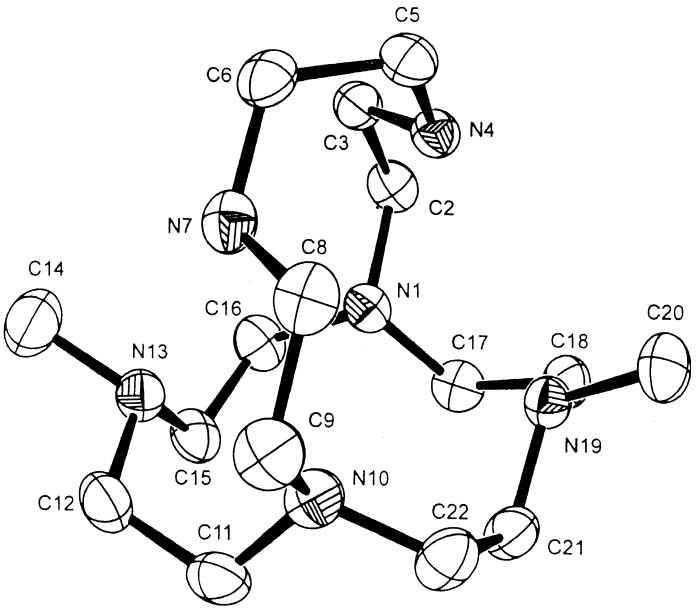

Figure 3. ORTEP diagram (50% probability) of $\mathbf{L}\cdot 2H_2O$. Hydrogen atoms have been omitted for clarity.

The crystal structure of $\mathbf{L}\cdot 2H_2O$, where hydrogen atoms have been omitted for clarity, is shown in Fig. 2 and the ORTEP diagram in Fig. 3.

The unit cell consists of one molecule of **L** hydrogen bonded to two molecules of water. Each ligand molecule interacts with two water molecules, as indicated by short contacts involving the oxygen atom of one water molecule O(24) and the secondary nitrogen atom N(7) and the oxygen atom of the second water molecule O(23) with the secondary nitrogen atom N(4), which are 2.782 and 2.835 Å, respectively. Both these distances fall into the expected range for N···H–O hydrogen bonds. Unfortunately, the quality of the data did not allow us to locate the positions of the hydrogen atoms of the water molecules to enable an accurate description of these interactions to be made.

Table 1. Bond distances (Å) and bond angles (°) for the metal coordination sphere of $[Li\mathbf{L}]^+[BPh_4]^{-*}$ and of $[Li\mathbf{L}]^+[ClO_4]^-$

$[Li\mathbf{L}]^+[BPh4]^-$		$[Li\mathbf{L}]^+[ClO4]^-$	
Bond distances			
N(246)–Li(4)	2.321(5)	N(10)*–Li	2187(6)
N(249)–Li(4)	2.205(6)	N(10)–Li	2.187(4)
N(253)–Li(4)	2.250(5)	N(4)–Li	2.262(4)
N(257)–Li(4)	2.359(5)	N(4)*–Li	2.262(4)
N(260)–Li(4)	2.318(6)	N(1)*–Li	2.349(4)
N(266)–Li(4)	2.266(6)	N(1)–Li	2.349(4)
Bond angles			
N(249)–Li(4)–N(253)	79.00(19)	N(10)*–Li–N(10)	79.90(3)
N(249)–Li(4)–N(266)	116.80(2)	N(10)*–Li–N(4)	117.19(14)
N(253)–Li(4)–N(266)	99.40(2)	N(10)–Li–N(4)	102.41(12)
N(249)–Li(4)–N(260)	104.10(2)	N(10)*–Li–N(4)*	102.41(12)
N(253)–Li(4)–N(260)	118.00(2)	N(10)–Li–N(4)*	117.19(14)
N(266)–Li(4)–N(260)	129.00(2)	N(4)–Li–N(4)*	128.00(3)
N(249)–Li(4)–N(246)	79.95(19)	N(10)*–Li–N(1)*	76.89(11)
N(253)–Li(4)–N(246)	156.40(2)	N(10)–Li–N(1)*	154.10(3)
N(266)–Li(4)–N(246)	80.70(2)	N(4)–Li–N(1)*	78.58(14)
N(260)–Li(4)–N(246)	77.60(2)	N(4)*–Li–N(1)*	79.23(15)
N(249)–Li(4)–N(257)	157.49(19)	N(10)*–Li–N(1)	154.10(3)
N(253)–Li(4)–N(257)	76.10(19)	N(10)–Li–N(1)	76.89(11)
N(266)–Li(4)–N(257)	79.00(2)	N(4)–Li–N(1)	79.24(15)
N(260)–Li(4)–N(257)	78.00(2)	N(4)*–Li–N(1)	78.58(14)
N(246)–Li(4)–N(257)	126.50(2)	N(1)*–Li–N(1)	127.90(3)

Asterisk (*) denotes that there are four crystallographically unique molecules in the unit cell.

The four basal nitrogen atoms are in the *endo* conformation with the ethylene carbon atoms below the basal plane, and the bridging nitrogen atoms are in an *exo* conformation. The bridge is perpendicular to the plane formed by the four basal nitrogen atoms, the bridging nitrogen atoms N(4) and N(7) exhibit weak hydrogen bonds with N(13) and N(19) [(N(4)–H···N(19) and N(7)–H···N(13) distances are 2.44 Å and 2.32 Å, respectively]. It is worth underlining that the Li–N(H) bond distances in this complex are significantly shorter that the Li–N(Me) distances as expected from coordination number considerations (see Table 1).

2.1. Crystal structure of $[LiL]^+$ $[BPh_4]^-$

The X-ray structure of the complex consists of discrete $[Li\mathbf{L}]^+$ cations and $[BPh_4]^-$ anions. Unfortunately an ORTEP diagram could not be obtained due to the fact that unit cell consists of more than 500 atoms. The crystal structure of $[Li\mathbf{L}]^+$ is shown in Fig. 4 and selected bond distances and bond angles are presented in Table 1.

From Fig. 4 we can see that the Li^+ is completely encapsulated in the macrobicycle and adopts a six coordinate geometry. There are four crystallographically unique molecules in the unit cell, differing in their bond distances and bond angles. The Li–N distances are in the range of 2.20–2.37 Å, which are comparable with those reported for noncaged[8] and caged[9,10] aza macrocycles of 2.11–2.45 Å.

2.2. Crystal structure of $[LiL]^+$ $[ClO_4]^-$

The structure of the compound consists of discrete $[Li\mathbf{L}]^+$ cations and distorted $[ClO_4]^-$ anions. The ORTEP diagram

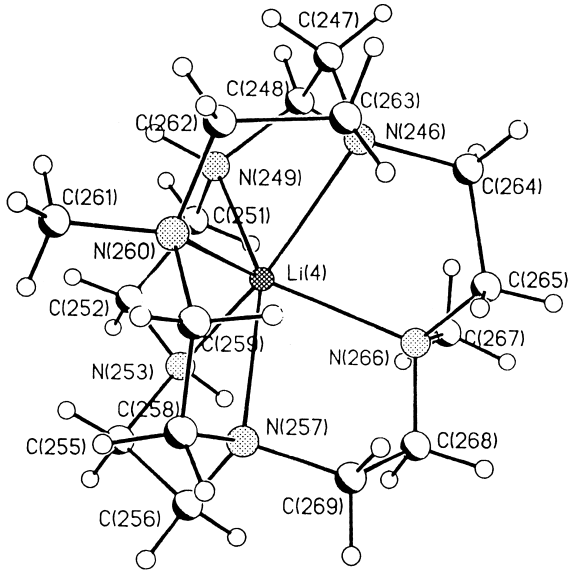

Figure 4. Crystal structure of $[LiL]^+[BPh_4]^-$. The labeling atoms correspond with one of the four molecules in the unique cell. Hydrogen atoms were omitted for clarity.

of $[LiL]^+$ cations is shown in Fig. 5 and bond distances and angles in Table 1.

The metal cation is also completely encapsulated in the cryptand and adopts a six coordinate geometry. The metal is located approximately 1.0156 (Å) above the basal plane that passes through the basal nitrogen atoms. The Li–N distances are in the range of 2.187–2.349 (Å). Like in the case of $[LiL]^+[BPh_4]^-$ crystal, the conformation of the bridge, comparative to that of the free ligand is changed, the lone pair electrons of the nitrogen atoms prefer to have an *endo* conformation due to metal ion encapsulation.

The ^{13}C NMR spectra of both encapsulated lithium complexes are identical and present four peaks (see Section 3).

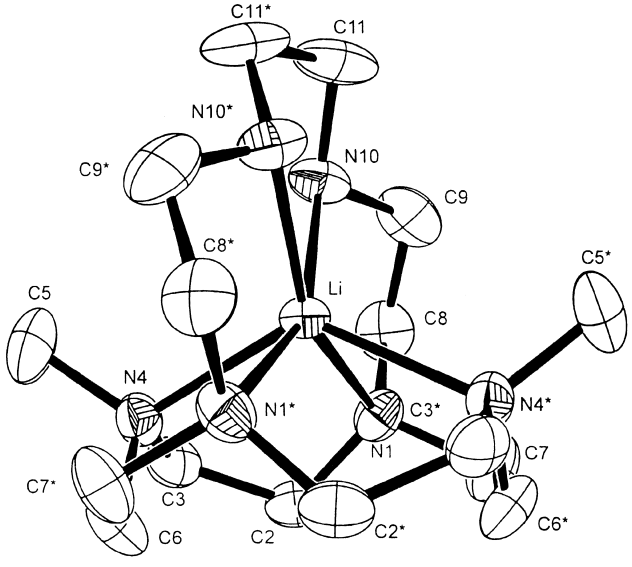

Figure 5. The ORTEP diagram (50% probability) of $[LiL]^+[ClO_4]^-$. The hydrogen atoms have been omitted for clarity.

3. Experimental

3.1. General

Melting points are uncorrected. The IR spectrum was recorded on a Perkin–Elmer Spectrum 200 instrument. The NMR spectra were recorded on a Varian, Gemini 300 spectrometer, in $CDCl_3$ (^{13}C NMR spectra of compounds **3**,**4** and **L**), in DMSO (^{13}C NMR spectra of **L**, of the encapsulated lithium complexes and ^1H NMR spectrum of **3**) or in CD_3OD (^1H NMR spectra of **L** and **4**) with tetramethylsilane as an internal reference. Mass spectra were performed with a Hewlett Packard Trio-1 spectrometer (EI=70 eV). Elemental analyses were performed on a Perkin–Elmer 2400 instrument.

Investigations on single crystals of **L**, $[LiL]^+$ $[BPh_4]^-$ and $[LiL]^+$ $[ClO_4]^-$ were carried out with a Siemens SMART CCD diffractometer with Mo Kα radiation (λ=0.71073).A summary of crystallographic data is reported in Table 2. The structures were solved by direct methods and refined by a full-matrix least-squares fit on F^2 using the SHELXTL package.[11] Absorption corrections were applied using SADABS. All non-hydrogen atoms were refined anisotropically. The molecular plots for **L** and for $[LiL]^+$ $[ClO_4]^-$ were produced by the program ORTEP.[12]

Crystals suitable for crystallographic structural determination were obtained by recrystallization of **L** from heptane and of $[LiL]^+$ $[BPh_4]^-$ and $[LiL]^+$ $[ClO_4]^-$ from a mixture of chloroform and cyclohexane.

Crystallographic data (excluding structure factors) for the structures reported in this paper have been deposited with the Cambridge Crystallographic Data Center as supplementary publication nos. CCDC 179642 (**L**), 179943 ($[LiL]^+$ $[BPh_4]^-$) and 179644 ($[LiL]^+[ClO_4]^-$). Copies of the data can be obtained free of charge on application to CCDC, 12 Union Road, Cambridge CB21EZ, UK (fax: +44-1223-336-033; e-mail; deposit@ccdc.cam.ac.uk).

3.1.1. 4,7-Dimethyl-15,18-ditosyl-1,4,7,10,15,18-hexaazabicyclo [8.5.5]octane (3). Finely powdered K_2CO_3 (17.5 g) was added to a solution of compound **1**[13] (4.58 g, 0.023 mol) in 250 mL of dry acetonitrile. The resulting solution was heated at reflux and a solution of **2**[14] (17.5 g, 0.023 mol) in 750 mL of dry acetonitrile was added dropwise over a period of 6 h and then refluxed for an additional 2 h. The solution was cooled, filtered and concentrated in vacuo to 80–90 mL. The precipitate was filtered and the rest of the solvent evaporated leaving behind a brown solid residue. This residue was triturated with ethanol and the white solid obtained was filtered. Both crops were united and recrystallized from ethanol. Yield 70.5%, mp=190–192 °C. MS (*m*/*z*): 622 (M^++2, 6), 621 (M^++1, 6), 620 (M^+, 12), 619 (M^+−1, 9), 618 (M^+−2, 14), 605 (M^+−15, 6), 594 (M^++2−28, 20), 593 (M^++1−28, 28), 592 (M^+−28, 100), 591 (M^+−8, 6), 578 (13), 577 (26), 576 (92), 575 (10), 565 (8), 564 (42), 563 (16), 562 (50). ^1H NMR (DMSO-d_6): 2.17 (6H, s, CH_3), 2.40 (6H, s, CH_3), 2.61 (8H, d, CH_2, *J*=4.6 Hz), 3.11 (8H, d, CH_2, *J*=4.3 Hz), 7.43 (4H, d, H aromatic, *J*=8.40 Hz), 7.71 (4H, d, H aromatic, *J*=7.8 Hz).^{13}C NMR, ($CDCl_3$): 21.42,

Table 2. X-Ray crystal data collection and refinement details for **L**, $[LiL]^+[BPh_4]^-$ and $[LiL]^+[ClO_4]^-$

	L	$[LiL]^+[BPh_4]^-$	$[LiL]^+[ClO_4]^-$
Formula	$C_{20}H_{30}N_8O_4$	$CH_{20}B_{0.19}Li_{0.19}N_8$	$C_{16}H_{30}ClLiN_6O_4$
FW	398.52	47.69	412.85
Crystal system	–	Triclinic	–
Space group	–	*P*1	–
a (Å)	9.0350(18)	15.616(3)	15.510(3)
b (Å)	9.5615(19)	15.722(3)	8.8055(18)
c (Å)	13.890(3)	23.920(5)	8.8090(18)
α (°)	79.99(3)	75.19(3)	90
β (°)	86.30(3)	88.72(3)	117.22(3)
γ (°)	63.10(3)	83.83(3)	90
T (K)	293(2)	173(2)	293(2)
V (Å^3)	1046.0(4)	5644.8(19)	1069.9(4)
Z	2	1	2
D_{calc} (mg m^{-3})	1.265	1.347	1.283
F(000)	428	2590	440
μ (mm^{-1})	0.084	0.100	0.211
θ range (°)	1.50–28.32	1.58–28.29	2.60–28.26
Index ranges	$-11<h<12$	$-20\le h<11$	$-20\le h\le 20$
	$-12<k<12$	$-20\le k\le 19$	$-11\le k\le 5$
	$-8\le l\le 18$	$-31\le l\le 31$	$-11\le l\le 11$
Reflection collected/unique	6690/4702	35825/29633	3436/1718
Data/restraints/parameters	4702/0/225	29633/3/2592	1718/1/164
Goodness-of-fit on F^2	1.205	0.699	0.960
Final R indices			
$[I>2\sigma(I)]$	*R*1=0.0486	*R*1=0.0465	*R*1=0.0470
	*wR*2=0.1550	*wR*2=0.1433	*wR*2=0.1244
R indices (all data)	*R*1=0.0594	*R*1=0.0747	*R*1=0.0631
	*wR*2=0.1611	*wR*2=0.1782	*wR*2=0.1346
Largest diff.	0.587	0.597	0.365
Peak and hole (e Å^{-3})	−0.200	−0.230	−0.225

43.36, 48.99, 49.46, 53.92, 55.11, 58.02, 127.41, 129.41, 136.74, 142.77. IR ($CHCl_3$): 3053, 2973, 2962, 2870, 2800, 1530, 1473, 1455, 1372, 1360, 1158, 835 cm^{-1}. Anal. calcd for $C_{30}H_{48}N_6S_2O_4$: C 58.04; H 7.79; N 15.54. Found: C 58.00; H 7.60; N 15.51.

3.1.2. 4,7-Dimethyl-1,4,7,10,15,18-hexaazabicyclo [8.5.5]-octane (L). 98% Sulphuric acid (9 mL) was added to compound **3** (5.58 g, 0.009 mol) and the mixture was stirred, under nitrogen at 100°C for 72 h. Then the solution was cooled in an ice bath and anhydrous diethyl ether (60 mL) was added slowly. The precipitated sulfate salt was filtered under nitrogen, washed with diethyl ether and dried in vacuo. Subsequently the salt was dissolved in water (20 mL) and NaOH solution (obtained from 4 g of NaOH and 10 mL of water) was added to neutralize the acid. The free base that precipitated was filtered, dried and dissolved in hexane. The resulting mixture was filtered and organic solvent evaporated. **L** was obtained as a white solid. Yield 70%, mp=98–100°C. Anal.calcd for $C_{16}H_{40}N_6O_2$: C 55.14; H 11.57; N 24.11. Found: C 56.80; H 12.00; N 24.50. MS (*m*/*z*): 313 (M^++1, 6), 312 (M^+, 24), 311 (M^+−1, 6), 297 (M^+−15, 6), 282 (M−30, 6), 281 (M^+−1−30, 9), 268 (42), 257 (15), 256 (100), 255 (15), 254 (70), 244 (14), 242 (91), 241 (8), 240 (36). ^{1}H NMR (CD_3OD-d_4): 2.21 (6H, s, CH_3), 2.32–2.54 (20H, overlapped peaks), 2.58–2.68 (4H, m), 2.70–2.76 (4H, m).^{13}C NMR (DMSO-d_6): 43.77, 47.00, 47.32, 52.45, 53.44, 55.44. Anal. calcd for $C_{16}H_{40}N_6O_2$: C 55.14; H 11.57; N 24.11. Found: C 56.80; H 12.00; N 24.50.

3.1.3. 4,7,15,18-Tetramethyl-1,4,7,10,15,18-hexaazabicyclo[8.5.5]octane (4). L (1.36 g, 0.42 mmol) was dissolved in formic acid (15 mL) with continuous stirring. A large excess of paraformaldehyde (4 g) was then added and the mixture refluxed for 24 h. Subsequently the reaction mixture was cooled, and the solvent evaporated when a yellow oil was obtained. To this oil, water (10 mL) was added and the solution made alkaline with solid KOH. The basic solution was extracted with CH_2Cl_2 (3×50 mL). The combined methylene chloride extracts were dried ($MgSO_4$) and solvent evaporated. The residue that results after evaporation was purified by column chromatography on neutral alumina with chloroform as the eluent. **4** was obtained as a colorless oil. Yield 65%. MS (*m*/*z*): 341 (M^++1, 6), 340 (M^+, 12), 339 (M^+−1, 7), 311 (7), 310 (10), 296 (29), 284 (79), 270 (100), 253 (17), 239 (76), 227 (86), 215 (64), 213 (93), 209 (83). ^{1}H NMR (CD_3OD-d_4); 2.18 (6H, s, CH_3), 2.30 (6H, s, CH_3) 2.43–2.65 (20H, overlapped peaks), 2.61–2.75 (4H, m), 2.84–2.87 (4H, m).^{13}C NMR ($CDCl_3$): 55.62, 55.14, 54.14, 53.50, 51.33, 42.18, 40.73. Anal. calcd for $C_{18}H_{42}N_6$: C 63.48; H 11.84; N 24.67. Found: C 63.50; H 12.00; N 24.83.

$[LiL]^+$ $[BPh_4]^-$ was obtained by refluxing a molar solution of **L** and $NaBPh_4$ with a 20-fold excess of LiOH in methanol (80 mL) for 1 h. On cooling,colorless crystals of $[LiL]^+$ $[BPh_4]^-$ slowly separated. ^{13}C NMR(DMSO-d_6): 42.70, 47.65, 49.39, 52.56, 121.43, 125.21, 135.48. Anal. calcd for $C_{40}H_{54}N_6BLi$: C 75.34; H 8.54; N 13.18. Found: C 75.00; H 8.79; N 12.98. *$[LiL]^+[ClO_4]^-$*.

A solution of LiOH (0.1 g, 4.16 mmol) and $NaClO_4$ (0.26 g, 2.12 mmol) in methanol (20 mL) was slowly added to a refluxing solution of **L** (0.6 g, 2 mmol) in methanol (20 mL). The mixture was refluxed for 30 min more, then cooled and the methanol was evaporated. The residue was

extracted with chloroform (10 mL), filtered and the complex was precipitated by the addition of cyclohexane. The crystals separated were filtered and dried. ^{13}C NMR (DMSO-d_6): 42.73, 46.71, 49.44, 52.60. Anal. calcd for $C_{16}H_{36}N_6O_4ClLi$: C 45.88; H 8.66; N 20.06. Found: C 46.00; H 8.75; N 20.50.

Acknowledgements

We thank NSF for the financial support, grant no. DMR-9988881.

References

1. (a) Dye, J. L. *Prog. Inorg. Chem.* **1984**, *32*, 327–441. (b) Dye, J. L. *Chemtrcats-Inorg. Chem.* **1993**, *5*, 243–270. (c) Cauliez, P. M.; Jackson, J. E.; Dye, J. L. *Tetrahedron Lett.* **1991**, *32*, 5039–5042. (d) Kuchenmeister, M. E.; Dye, J. L. *J. Am. Chem. Soc.* **1989**, *111*, 935–938. (e) Huang, R. H.; Huang, S. Z.; Dye, J. L. *Coord. Chem.* **1998**, *46*, 13–31. (f) Dye, J. L.; Ceraso, J. M.; Lok, M. T.; Barnett, B. L.; Tehan, F. J. *J. Am. Chem. Soc.* **1974**, *96*, 608–609. (g) Tehan, F. J.; Barnett, B. L.; Dye, J. L. *J. Am. Chem. Soc.* **1974**, *96*, 7203–7208.
2. Eglin, J. L.; Jackson, E. P.; Moeggenborg, K. J.; Dye, J. L.; Bencini, A.; Micheloni, M. *J. Incl. Phenom. Mol. Recognit. Chem.* **1992**, *12*, 263–274.
3. Cahen, Y.; Dye, J. L.; Popov, A. I. *J. Phys. Chem.* **1975**, *79*, 1292–1295. Shamsipur, M.; Popov, A. I. *J. Phys. Chem.* **1986**, *90*, 5997–5999.
4. Bencini, A.; Bianchi, A.; Cimichi, S.; Ciampolini, M.; Dapporto, P.; Garcia-Espana, E.; Micheloni, M.; Nardi, N.; Paoli, P.; Valtancoli, B. *Inorg. Chem.* **1991**, *30*, 3687–3691.
5. Benicni, A.; Bianchi, A.; Borseli, A.; Ciampolini, M.; Micheloni, M.; Nardi, N.; Paoli, P.; Valtancoli, B.; Chimichi, S.; Dapporto, P. *J. Chem. Soc., Chem. Commun.* **1990**, 174–175.
6. Izatt, R. M.; Bradshaw, J. S.; Nielsen, S. A.; Christensen, J. P.; Sen, D. *Chem. Rev.* **1985**, *85*, 271–339.
7. Pross, A. *Theoretical and Physical Principles of Organic Reactivity*; Wiley: New York, 1995; pp 202–204.
8. Constable, E. C.; Chung, L. Y.; Lewis, J.; Raithby, P. *J. Chem. Soc., Chem. Commun.* **1986**, 1719–1720.
9. Bencini, A.; Bianchi, B.; Borseli, E.; Ciampolini, M.; Garcia-Espana, E.; Dapporto, P.; Micheloni, M.; Paoli, P.; Ramirez, J. A.; Valtancoli, B. *Inorg. Chem.* **1989**, *28*, 4279–4284.
10. Bencini, A.; Bianchi, B.; Ciampolini, M.; Garcia-Espana, E. *J. Chem. Soc.,Chem. Commun.* **1989**, 701–703.
11. *Structure Analysis Program 5.1*; Brucker AXS, Inc.: Madison, WI, 1997.
12. Johnson C. K. *ORTEP; Report ORNL-3794*; Oak Ridge National Laboratory: Oak Ridge, TN, 1971.
13. Ciampolini, M.; Micheloni, M.; Nardi, N.; Paoleti, P.; Dapporto, P.; Zanobibi, F. *J. Chem. Soc., Dalton Trans.* **1984**, 1357–1362.
14. Kovacs, Z.; Archer, A.; Russell, M. K.; Sherry, A. D. *Synth. Commun.* **1999**, *29*, 2817–2822.